THE JOURNAL OF BIOLOGICAL CHEMISTRY VOL. 287, NO. 44, pp. 37089–37097, October 26, 2012

Global Identification of New Substrates for the Yeast Endoribonuclease, RNase Mitochondrial RNA Processing (MRP)*[S]

Received for publication, June 6, 2012, and in revised form, September 11, 2012 Published, JBC Papers in Press, September 12, 2012, DOI 10.1074/jbc.M112.389023

Jason Aulds[‡], Sara Wierzbicki[‡], Adrian McNairn[‡§], and Mark E. Schmitt[‡1]

From the [‡]Department of Biochemistry and Molecular Biology, State University of New York Upstate Medical University, Syracuse, New York 13210 and [§]Department of Biomedical Sciences, College of Veterinary Medicine, Cornell University, Ithaca, New York 14853

Background: A global RNase MRP substrate hunt has never been performed.
Results: We identified new potential substrates for RNase MRP.
Conclusion: Results confirm a role for RNase MRP in the cell cycle and identify new roles in the biosynthesis of other RNA-protein complexes.
Significance: Knowing the identity of RNase MRP substrates is critical to understanding its function and role on a system-wide scale.

RNase mitochondrial RNA processing (MRP) is an essential, evolutionarily conserved endoribonuclease composed of 10 different protein subunits and a single RNA. RNase MRP has established roles in multiple pathways including ribosome biogenesis, cell cycle regulation, and mitochondrial DNA replication. Although each of these functions is important to cell growth, additional functions may exist given the essential nature of the complex. To identify novel RNase MRP substrates, we utilized RNA immunoprecipitation and microarray chip analysis to identify RNA that physically associates with RNase MRP. We identified several new potential substrates for RNase MRP including a cell cycle-regulated transcript, *CTS1*; the yeast homolog of the mammalian p27^{Kip1}, *SIC1*; and the U2 RNA component of the spliceosome. In addition, we found RNase MRP to be involved in the regulation of the Ty1 transposon RNA. These results reinforce and broaden the role of RNase MRP in cell cycle regulation and help to identify new roles of this endoribonuclease.

RNase mitochondrial RNA processing (MRP)[2] is a highly conserved and essential endoribonuclease enzyme complex present in all eukaryotes with known functions in mitochondrial DNA replication, ribosomal biosynthesis, and cell cycle regulation. The yeast RNase MRP is composed of 10 protein subunits and a 340-nucleotide RNA encoded by the *NME1* gene, all of which are essential for viability. It shares eight of these proteins (Pop1p, Pop3p, Pop4p, Pop5p, Pop6p, Pop7p, Pop8p, and Rpp1) with the evolutionarily related RNase P, an endoribonuclease responsible for cleaving tRNA at its 5′-end as a normal part of the tRNA maturation process (1–4).

RNase MRP is found predominately localized to the nucleolus where it processes preribosomal RNA at the A3 site, leading to formation of the more abundant 5.8 S short ribosomal RNA (5, 6). RNase MRP is also present in the cytoplasm where it participates in cell cycle regulation (7–9) and within the mitochondria where it is proposed to be required for transcription-dependent mitochondrial DNA replication by cleaving a mitochondrial transcript RNA to form the replication primer (10, 11).

RNase MRP mutants exhibit a mitotic cell cycle delay characterized by the formation of large budded cells, an hourglass-shaped nucleus that is split between mother and daughter cells, and a long mitotic spindle (7). The increased spindle stability in these mutants is caused by elevated levels of the B-type mitotic cyclin Clb2p, resulting in the extended activity of the Clb2p/Cdc28p cyclin kinase pair and consequently an extended mitosis (9). *In vitro* and *in vivo* analyses showed that RNase MRP directly cleaves the 5′-untranslated region (UTR) of *CLB2* mRNA in a site-specific manner, facilitating its rapid degradation by the 5′ to 3′ exoribonuclease Xrn1p (9). Human cells with a mutation in the gene encoding the human RNase MRP RNA (RMRP) have been shown to display a similar molecular defect in cyclin mRNA processing and rRNA processing (12, 13).

In yeast, RNase MRP colocalizes with Xrn1p in the cytoplasm of the daughter cell during mid-to-late mitosis in a pattern characterized by small punctate foci (temporal asymmetric MRP (TAM) bodies) that appear during anaphase. They are transported in a Myo4p-dependent manner to the cytoplasm of the daughter cell where they persist until cytokinesis (8). The localization of these foci is conditional on RNase MRP function, and they are proposed to be the sites of mRNA processing by RNase MRP and subsequent degradation by Xrn1 (8).

To determine whether RNase MRP has additional RNA substrates, we utilized TAP-tagged RNase MRP protein Rmp1 to affinity capture RNase MRP and its substrates. As the endori-

* This work was supported, in whole or in part, by National Institutes of Health Grant GM063798 from the NIGMS.
[S] This article contains supplemental Fig. 1.
[1] To whom correspondence should be addressed: Dept. of Biochemistry and Molecular Biology, State University of New York Upstate Medical University, 750 E. Adams St., Syracuse, NY 13210. Tel.: 315-464-8713; Fax: 315-464-8750; E-mail: schmittm@upstate.edu.
[2] The abbreviations used are: MRP, mitochondrial RNA processing; RIP-chip, RNA immunoprecipitation and microarray chip analysis; TAP, tandem affinity purification; RMRP, RNase MRP RNA; TAM, temporal asymmetric MRP.

bonuclease activity of the enzyme requires the physical association of the substrate with the enzyme, captured RNAs outside of the MRP RNA are expected to be candidate substrates. We identified the captured RNAs using oligonucleotide microarrays for *Saccharomyces cerevisiae*. We have modified this approach by subjecting the cells to ultraviolet light prior to lysis to covalently bind substrate RNA to the RNase MRP complex and thus increase the RNA substrate yield (14, 15). We have called this procedure RNA immunoprecipitation and microarray chip analysis (RIP-chip) (15). This methodology enabled us to identify several new RNase MRP substrates including *CTS1*, *SIC1*, *LSR1* and to identify a role for RNase MRP in the Ty1 retrotransposon cycle.

EXPERIMENTAL PROCEDURES

Analysis of Yeast RNA—Extraction of RNA was performed as described previously (16). Separation and analysis of total RNA were performed as described (17) for both urea denaturing polyacrylamide and formaldehyde denaturing agarose gels. Northern blot analysis was performed as described (5). All DNA probes used were made by polymerase chain reaction (PCR) using the following primers: CTS1-F1 (AAA AAC CTC AGC AGC CTC AA), CTS1-R1 (GAA CTT CCC ATC AGC AGA GC), SIC1-F1 (GCC CTA ATG CAA GGT CAA AA), SIC-R1 (GAC TCC TGG CGT CAT TTT C), LSR1-F (CGG CCA AAG TTG TTG ATT TT), LSR1-R (GCA TTC TTC AAA TCC CTC CA), 5′-TERCTY1-2 (AAT GCA ATC TGA TAC CCA AGA GGC), 3′-TERCTY1-2 (GAT AGG TGC AAG TAC AGT GCC GTC), VPH1F1 (ATA TTT GGA CGG CTC AGG TG), VPH1-R1 (TGT GGG TAA A CCA GCA TTG A), SCR1-F (TGA TCA ACT TAG CCA GGA C), SCR1-R (GAT CAA CTT GCA CAA TTA T), CTS1-F3 (GCG GCC GCC AAT TTA GGT GAC ACT ATA GGA ATG GAC AAC AAC AAT ACA TTA C), and CTS1-R3 (GGA TCC GAA GAA TGA TGT AAA GGA GTG ACA. Probes were radiolabeled with [^{32}P]dCTP using the Prime-It II kit (Stratagene, Inc., La Jolla, CA) and purified by gel exclusion chromatography using G-50 Sephadex as described (17). Radioactive blots were analyzed on a GE Healthcare/Amersham Biosciences Typhoon variable mode imager. For Northern analysis, yeast strains were all grown at 28 °C to late log phase and moved to 37 °C for 2 h prior to harvesting cells for RNA.

In Vitro Cleavage Assay—The RNase MRP cleavage assays and the generation of 3′-end-labeled substrates were performed as described previously (9) using the pJA110 template for the A3 cleavage as a positive control. The template for the *CTS1* substrate was generated by PCR amplification of the 5′-UTR of the *CTS1* gene with a 5′ primer bearing an SP6 polymerase promoter (CTS1-F3) and a 3′ primer bearing a BamHI site (CTS1-R3). This fragment was cloned into the pRS315 vector and digested with BamHI for the synthesis of RNA with SP6 RNA polymerase. The substrate RNA is ~265 nucleotides.

Purification of RNase MRP—RNase MRP was purified from *S. cerevisiae* with the tandem affinity purification (TAP) tag protocol as described (1). The Rmp1 TAP-tagged strain used in this manuscript is KLS116 (1).

Primer Extension—Primer extension was carried out as described previously (9) with CTS1-R3 oligonucleotide labeled with [^{32}P]ATP and polynucleotide kinase on its 5′-end. The same primer was used in a DNA sequencing reaction and run in parallel on a sequencing gel as described (9).

Cell Synchronization and RNA Analysis—Erlenmeyer flasks containing 350 ml of synthetic complete dextrose (9) medium were each inoculated with isogenic strains carrying either the *nme1-Δ2* allele or the wild-type *NME1* allele to a density of 2.0×10^6 cells/ml. The cultures were incubated at 28 °C and shaken until the densities reached 1.5×10^7 cells/ml. At that time, 25 ml of 210 mg/ml hydroxyurea (Arco; 99% pure) was added into each culture and incubated an additional 3 h whereupon cells were collected at 5000 rpm for 5 min at 28 °C and washed four times with 35 ml of 28 °C synthetic complete dextrose each time. Cells were suspended in 35 ml of 28 °C synthetic complete dextrose, inoculated into 350 ml of synthetic complete dextrose, and incubated at 31 °C. From these cultures, we collected 25 ml of cells at 15-min intervals from 0 to 180 min. Cell density was determined every 30 min using a hemocytometer. For each time point, cells were photographed from the most representative field for each culture at each time fraction using 450× magnification with the differential interference contrast setting. After collection at each time point, cells were immediately stored at −80 °C.

UV Cross-linking and Affinity Purification of RNase MRP Complex with Substrate—Erlenmeyer flasks containing 500 ml of yeast extract/peptone/dextrose medium were inoculated at 2.5×10^6 cells/ml and incubated with shaking at 28 °C for 8 h until they reached a density of around 5.0×10^7 cells/ml. We performed UV irradiation by quickly transferring all of each culture to 12 × 22-inch glass trays and irradiating cells for two 2-min intervals at 254 nm in a Stratagene Corp. Stratalinker (~930 mJ/cm^2). Cultures were stirred between irradiations and collected at 5000 × *g* for 5 min at 4 °C. Cells were then washed in chilled water twice, collected as before, and stored at −80 °C until lysis. Purification of RNase MRP with substrate was carried out as described previously (1) except that the calmodulin affinity column was not used. Instead, the tobacco etch virus protease elution was directly extracted as described below.

Proteinase K Treatment and Phenol/Chloroform Extraction—To the tobacco etch virus protease elution we added 20% SDS to a final concentration of 5% (v/v) and 2-mercaptoethanol to 10% (v/v) and then heated the sample to 95 °C for 10 min. We allowed the samples to cool to room temperature, $CaCl_2$ was added to a final concentration of 5 mM, and Proteinase K was added to final a concentration of 100 μg/ml. The sample was incubated at 50 °C for 1 h followed by 95 °C for 5 min to inactivate the Proteinase K. Phenol/chloroform extraction and ethanol precipitation of RNA were then performed as described (18). RNA pellets were suspended with 200 μl of diethyl pyrocarbonate-treated double distilled H_2O. RNA concentration and quality were determined by UV spectrophotometric analysis at 260 and 280 nm. Samples were run through an Agilent bioanalyzer on an RNA nanochip for qualitative analysis.

Microarray Analysis—Microarray analysis was performed in the State University of New York Upstate Medical University Microarray Core Facility using Affymetrix Yeast Genome S98 arrays. For RNA labeling, 100 ng of total RNA was amplified using Ovation RNA Amplification System V2 from NuGEN

Technologies. The cDNA generated from this protocol was fragmented and biotin-labeled using the Encore Biotin Module. Each labeled cDNA sample was then hybridized to a microarray with incubation at 45 °C in Affymetrix Hybridization Oven 645. After 18 h of incubation, the arrays were processed in Affymetrix Fluidics Station 450 using reagents from Affymetrix and standard protocols. Arrays were scanned with Affymetrix GeneChip Scanner 7G Plus.

RESULTS

To identify novel RNase MRP substrates, we utilized a previously characterized strain expressing an Rmp1 TAP-tagged allele, KLS116 (1). Yeast cells were cross-linked with UV irradiation as described under "Experimental Procedures," the RNase MRP enzyme was immunoprecipitated using the TAP tag, and co-purifying RNAs were isolated and hybridized to a DNA microarray. The data were parsed in two different ways: by a call on whether it was present or absent and by an overall change in signal level over an untagged control strain. A probe proximal to a well characterized RNase MRP cleavage site in the rRNA precursor was found to be overrepresented 17.38-fold over control. Hence, we made this the cutoff for a significant hit. Remaining were 70 positive probes that were found to be overrepresented from 17.7- to 210-fold over control. These represented 64 unique ORFs (Table 1

Many of these co-precipitating RNAs were encoded by ribosomal protein genes, but there were several groups of RNAs identified whose products are involved in other aspects of protein synthesis. However, most abundant in terms of hybridization signal were ribosomal protein transcripts. This abundance may be an artifact of their high abundance in a cell; however, levels of these transcripts were considerably lower or absent in the untagged strain. In addition to transcripts whose product is involved in translation, we encountered a small group of cell cycle-regulated transcripts.

Validation of Individual RNAs from the RIP-chip Data Set—To verify whether or not the individual RNAs identified by microarray analysis were indeed RNase MRP substrates, we first determined whether the steady-state level of each RNA was altered in RNase MRP mutants. Compared with wild-type cells, RNase MRP mutants exhibit decreased RNA processing ability, resulting in an increase in the stability and hence the amount of substrate RNA in the cell. This relative increase of substrate RNA in RNase MRP mutants compared with wild-type cells can be measured most effectively by Northern blot analysis. We selected several RNAs with elevated signals from the RIP-chip analysis: *RPL31b*, *RPL34a*, *STM1*, and *LSR1* were chosen based on their exceptionally high hybridization levels; *CTS1*, *SIC1*, and *HTB1* were selected as representative cell cycle-regulated transcripts; *NOP1* was selected as representative of rRNA processing; and Ty1 RNA was examined because of the multiple hits we received with it. We choose four different RNase MRP mutant strains to examine RNA levels. Two of the mutants contained different temperature-sensitive alleles of the RNase MRP RNA, *nme1-P6* and *nme1-Δ2* (19), and two contained different temperature-sensitive alleles of a unique RNase MRP protein component, *snm1-172* and *snm1-P18* (18).

Total RNA was collected from all four yeast strains along with wild-type controls. RNA was separated, blotted, and probed using DNA probes specific for each mRNA. The steady-state mRNA levels of *RPL31b*, *RPL34a*, *HTB1*, *NOP1*, and *STM1* showed only modest changes in the mutant strains as compared with the wild-type strains (data not shown). These results indicate that although these transcripts may associate with RNase MRP they are not necessarily substrates of the enzyme. In contrast, Northern blot analysis of *SIC1*, *LSR1*, and *CTS1* indicated an increase in RNA levels consistent with RNase MRP playing a role in their degradation (Fig. 1).

SIC1 mRNA Is Elevated in RNase MRP Mutants—SIC1, the yeast homolog of the $p27^{Kip1}$ cyclin-dependent kinase inhibitor, is a key regulator of mitotic exit and Clb2p abundance. Human p27 has been implicated in cell cycle deregulation and cancer development (20). *SIC1* is expressed in a manner similar to but slightly later than *CLB2* mRNA and is enriched >2-fold in RNase MRP mutants as determined by Northern blot analysis (Fig. 1*A*). Furthermore, a *sic1Δ*/*nme1-p6* double mutant exhibits a synthetic growth defect, indicating a genetic interaction likely due to their roles in reducing Clb2 activity (Fig. 2*A*). The elevated *SIC1* mRNA levels and its association with Rmp1 strongly suggest that it is an RNase MRP substrate and indicate that RNase MRP may have additional roles in fine tuning mitotic exit.

LSR1 Levels Are Increased in RNase MRP Mutants—LSR1, the U2 snRNA and integral component of the spliceosome required for splicing of intron-bearing transcripts, exhibited a significant enrichment in the RIP-chip analysis. Northern analysis showed an elevation of *LSR1* RNA levels in MRP mutants as compared with wild-type cells, indicating that RNase MRP may function in the assembly or degradation of this RNA (Fig. 1*C*). We directly tested for genetic interactions between the *nme1-P6* mutation and two non-essential protein components of the U2 small nuclear ribonucleoprotein, Msl1 and Lea1. Msl1 and Lea1 are the U2B component and U2A component of the U2 small nuclear ribonucleoprotein, respectively (21). Double mutants containing either *msl1Δ*/*nme1-p6* or *lea1Δ*/*nme1-p6* were found to be slow growing (Fig. 2*B*). We also found that deletion of *DBR1*, the gene for the debranching enzyme that resolves the excised intron lariat (22), is growth-defective in combination with *nme1-p6* (Fig. 2*B*). In addition, a deletion of the gene for the pseudouridine synthase, Pus7, which is necessary for the proper pseudouridylation of U2 RNA (23), exhibits a genetic interaction with RNase MRP (Fig. 2*B*). The detection of U2 RNA associated with Rmp1, the elevated U2 RNA levels in RNase MRP mutants, and the genetic interactions between RNase MRP components and U2 components strongly suggest a direct association between U2 RNA and RNase MRP.

CTS1 mRNA Is Elevated in RNase MRP Mutants—CTS1 encodes an endochitinase required for the degradation of the primary septum during cytokinesis. Northern blot analysis of *CTS1* mRNA in *nme1-Δ2*, *nme1-p6*, *snm1-172*, and *snm1-p18* strains as compared with their respective wild-type strains indicated that it is elevated in all RNase MRP mutants (Fig. 1*B*). Interestingly, *CTS1* mRNA levels in *nme1-Δ2* are considerably higher than in the other three mutants. This could partially be

TABLE 1

RNAs identified to be associated with the TAP-tagged version of Rmp1

Fold overrepresented indicates the ratio of signal from the Rmp1 tagged strain *versus* the untagged strain. Genes are shown in gene ontology groups. SAGE, *serial analysis of gene expression; ER, endoplasmic reticulum; LSU, large subunit.*

Affymetrix probe set	Gene	Average -fold overrepresented	Description	Comments
Protein synthesis and ribosome biogenesis				
5670_i_at	*RPL34A*	210.6	YER056C-A	
9897_f_at	*RPL31B*	178.4	YLR406C	
4909_f_at	*RPS23A*	87.6	YGR118W	
7707_i_at	*RPL43A*	71.1	YPR043W	
7633_s_at	*RPL11A*	67.0	YPR102C	
6069_i_at	*RPL12B*	63.7	YDR418W	
10386_s_at	*RPL8B*	63.4	YLL045C	
4165_i_at	*RPL34B*	59.6	YIL052C	
5985_at	*RPL27B*	59.5	YDR471W	
5075_i_at	*RPL7A*	57.3	YGL076C	
10783_at	*SNR190*	50.4	SNR190; small nuclear RNA190	C/D box LSU G2395
5076_f_at	*RPL7A*	47.9	YGL076C	
8054_at	*SNR50*	43.6	SNR50 snRNA	C/D box LSU G867
10387_at	*YLL044w*	41.1	YLL044W; questionable ORF	Overlaps with RPL8B
5142_i_at	*RPL9A*	38.4	YGL147C	
6866_at	*RPS14A*	36.6	YCR031C	
8270_f_at	*RPS10A*	36.0	YOR293W	
8246_s_at	*YOR309C*	35.5	YOR309C	Overlaps with Nop58
6493_at	*NOP1*	34.1	YDL014W	
9691_i_at	*RPS1B*	33.8	YML063W	
10739_f_at	*RPL17A*	33.4	YKL180W	
7454_s_at	*RPL23A*	32.1	YBL087C	
6672_s_at	*RPL35A*	31.4	YDL191W	
9193_at	*SNR73*	27.9	SNR73; snRNA	C/D box position C2959
9176_at	*KRI1*	27.1	YNL308C	rRNA processing
4528_i_at	*RPL27A*	25.7	YHR010W	
9496_at	*RPL13B*	25.0	YMR142C	
7316_s_at	*RPS11B*	24.8	YBR048W	
10707_at	*SRP21*	22.3	YKL122C; component of signal recognition particle	
6070_s_at	*RPL12B*	21.8	YDR418W	
10717_at	*RPS27A*	21.2	YKL156W	
7806_at	*EGD1*	20.8	YPL037C; associated with ribosomes	
8879_at	*PUB1*	20.1	YNL016W; poly(A)$^+$ RNA-binding protein	
7656_s_at	*TEF1*	20.0	YPR080W; translational elongation factor EF-1α	
5807_at	*SNR13*	20.0	SNR13; snRNA	C/D box LSU A2280
7191_f_at	*RPS9B*	19.9	YBR189W	
11205_i_at	*RPL17B*	19.8	YJL177W	
4771_at	*NOP19*	19.3	YGR251W	rRNA processing
4516_f_at	*RPL14B*	17.8	YHL001W	
6895_at	*SRO9*	17.7	YCL037C; RNA binding associated with ribosome	
3808_s_at	*ITS1*	17.4	RDN37-1; 35 S ribosomal RNA	
Ty elements				
3781_f_at		66.4	YLRWTY1-2; full length Ty1	
3350_f_at		50.7	YERCTY1-1; full length Ty1	
3786_s_at		42.9	Ty1B protein	
Cell cycle				
6301_at	*CPR1*	85.9	YDR155C; cyclophilin	
10045_at	*CTS1*	67.9	YLR286C; endochitinase	
6235_at	*HTB1*	28.4	YDR224C; histone H2B	
7369_s_at	*HHT1*	23.0	YBR010W; histone H3	
10243_at	*SIC1*	20.9	YLR079W; p40 inhibitor of Cdc28	
4233_at	*SIM1*	20.8	YIL123W; involved in cell cycle regulation and aging	
7245_at	*CMD1*	19.6	YBR109C; calmodulin	
Metabolism				
11031_s_at	*TDH2*	105.2	YJR009C; glyceraldehyde-3-phosphate dehydrogenase	
9979_at	*ILV5*	71.6	YLR355C; acetohydroxyacid reductoisomerase	
8973_at	*LEU4*	37.9	YNL104C; α-isopropylmalate synthase	
4856_at	*CYS4*	23.2	YGR155W; cystathionine β-synthase	
7689_at	*SPE3*	20.3	YPR069C; putrescine aminopropyltransferase	
4499_at	*THR1*	20.0	YHR025W; homoserine kinase	
4321_at	*BAT1*	19.8	YHR208W; branched-chain amino acid transaminase	
7152_at	*PGI1*	18.9	YBR196C; glucose-6-phosphate isomerase	

TABLE 1—*continued*

Affymetrix probe set	Gene	Average -fold overrepresented	Description	Comments
Others				
6954_at	*LSR1*	140.0	LSR1; U2 snRNA	
10180_at	*STM1*	75.7	YLR150W; specific affinity for G-rich quadruplex nucleic acids	
7290_at	*TIP1*	47.7	YBR067C; cell wall mannoprotein	
6324_g_at		40.6	YDR133C; questionable ORF	
4709_at	*SCW4*	38.2	YGR279C; glucanase gene family member	
5553_at	*BUR6*	34.8	YER159C; transcriptional regulator	
4526_at	*SOD2*	29.3	YHR008C; manganese-containing superoxide dismutase	
4561_s_at	*SNR7-L*	26.2	SNR7-L; U5 snRNA	
5923_at		25.4	YDL085c-a; identified by SAGE	
4751_at	*PHB2*	24.8	YGR231C; mitochondrial protein; prohibitin homolog	
5268_at	*GUS1*	24.0	YGL245W; glutamine-tRNA ligase	
8935_at	*COX5a*	23.7	YNL052W; cytochrome-*c* oxidase chain Va	
5709_at	*NTF2*	23.4	YER009W; nuclear import	
8314_g_at	*SRL1*	22.7	YOR247W; mannoprotein associated with the cell wall	
9974_at	*ORM2*	22.6	YLR350W	
3949_i_at	*YIP3*	22.5	YNL044W; ER to Golgi vesicle-mediated transport	
10954_at	*LIA1*	21.9	YJR070C; deoxyhypusine hydroxylase	
6410_at	*SSS1*	18.7	YDR086C; part of the Sec61 trimeric complex	
7639_at	*RPN7*	18.5	YPR108W; subunit of the regulatory particle of the proteasome	
5728_i_at	*PMP2*	18.1	YEL017C-A; proteolipid with plasma membrane H^+-ATPase	

due to the general catalytic activity of RNase MRP being more impaired or alternatively to a loss of substrate specificity for *CTS1* mRNA in this mutant. *CTS1* has previously been identified as having a long 5′-UTR (217–231 nucleotides) analogous to the *CLB2* mRNA, the first identified mRNA substrate of RNase MRP (9, 24, 25).

To determine whether this region of the *CTS1* mRNA can be processed by RNase MRP, we performed a cleavage assay whereby we subjected *in vitro* transcribed RNA containing the *CTS1* 5′-UTR to RNase MRP enzyme purified from yeast (Fig. 3*A*). The *CTS1* 5′-UTR substrate was cleaved at a rate equivalent to that of the 5.8 S rRNA A3 substrate. Similar to the *CLB2* substrate, multiple cleavage sites were seen (9). To establish the exact sites of RNase MRP cleavage on the *CTS1* 5′-UTR, we performed primer extension analysis to map the cleavage sites. As can be seen (Fig. 3*B*), nine sites were identified throughout the transcript. These sites appear to be a collection of five major sites accompanied by some minor sites. The cleavage profile as indicated was invariable throughout several assays, indicating a degree of specificity in substrate cleavage (Fig. 3*B*). The RNase MRP cleavage profile of *CTS1* and *CLB2* suggests that the enzyme works in a processive manner, establishing recognition and cleaving the substrate repeatedly (Fig. 3*B* and Ref. 9). This manner of cleavage is similar to what has been reported in mouse nuclear RNase MRP enzyme cleavage of mitochondrial substrate (26, 27). A search for consensus sites in known substrates revealed no compelling recognition sequence. However, the first cleavage site does match the ↓CUC consensus seen previously (Ref. 28 and supplemental Fig. 1).

CTS1 Levels Do Not Return to Normal Levels after M Phase in an RNase MRP Mutant—The hallmark of deregulation of a cell cycle-regulated transcript is a failure to return to normal levels after peak expression. To determine whether the levels of *CTS1* are affected in an RNase MRP mutant, wild-type and mutant cells were synchronized with hydroxyurea and released, and RNA was collected at various time points after release. As is the case with *CLB2* mRNA deregulation in an *nme1-p6* mutant (9), *CTS1* mRNA levels peak normally during mitosis but fail to cycle back down in an *nme1-Δ2* mutant as compared with wild type (Fig. 4*A*). *CTS1* is temporally regulated to trigger the degradation of the primary septum following chromosomal segregation for cytokinesis to occur (29). This temporal regulation may be affected in RNase MRP mutants due to extended transcript stability.

CTS1 mRNA Degradation Requires Both RNase MRP and Xrn1—Having established that *CTS1* mRNA is a substrate for RNase MRP, we sought to determine whether *CTS1* mRNA stability is Xrn1-dependent like the *CLB2* mRNA (9). By comparing *CTS1* mRNA levels in *nme1-Δ2*, *Δxrn1*, *nme1-Δ2*/*Δxrn1*, and wild-type strains, we found that *CTS1* mRNA stability is greater in the double mutant compared with either single mutant or the wild-type strain (Fig. 4*B*). This suggests that *CTS1* mRNA is targeted for degradation by the Xrn1 exoribonuclease following RNase MRP cleavage in its 5′-UTR. This result suggests that the degradation of the *CTS1* mRNA occurs in TAM bodies by RNase MRP and Xrn1 in a manner identical to *CLB2* mRNA (8).

Ty1 RNA Elements Associate with Rmp1 and Are Reduced in RNase MRP Mutants—Ty1 elements are yeast retrotransposons that make up a significant portion of the yeast genome and are typically dormant for transposition. Their replication is cell cycle-regulated, and unlike Ty3 elements, they transpose in a manner that is almost universally dependent on tRNA proximity (30). Ty1 is among the most abundant RNAs found to associate with Rmp1. Unexpectedly, Northern analysis of Ty1 RNA from time fractions of synchronized cells indicated that

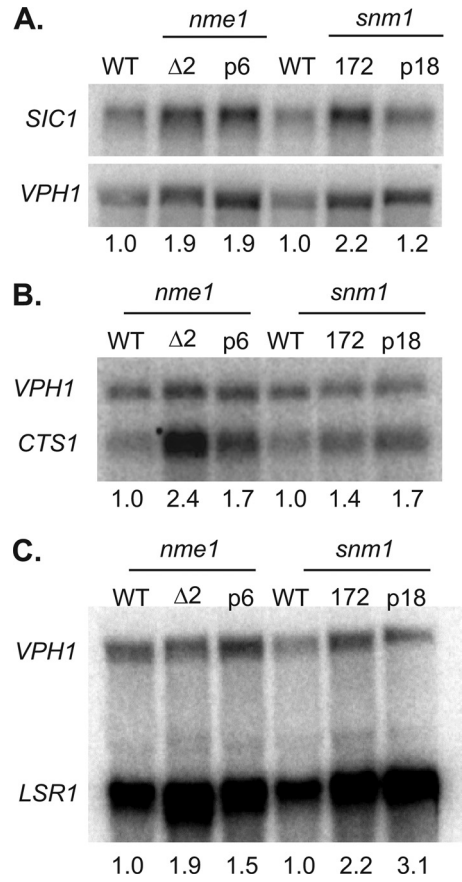

FIGURE 1. **Northern blot analysis of potential targets in wild-type and RNase MRP mutants.** Total RNA from wild-type and RNase MRP mutant cells was separated on a formaldehyde-agarose denaturing gel, transferred, and probed for *VPH1* mRNA (control) and either *SIC1* (*A*), *CTS1* (*B*), or *LSR1* (*C*). RNA levels for each sample were normalized to the loading control *VPH1* RNA and to the wild type as measured using ImageQuant 5.0 image analysis software. Wild type was given a relative value of 1.0. Calculated values are listed under each set of gels.

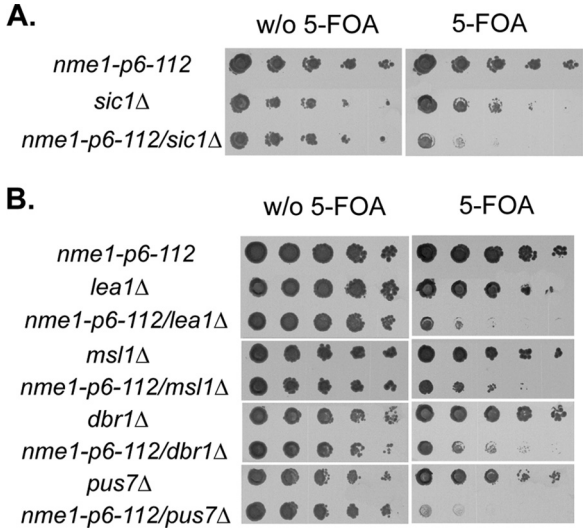

FIGURE 2. **Genetic interaction between cleavage targets and RNase MRP.** The indicated mutant yeast strains were serially diluted and replica-pinned onto either synthetic dextrose (−Ura) plates or 5-flouroorotic acid (*5-FOA*) plates. The cells in each of the cultures contain a plasmid with a *URA3* marker and wild-type copy of *NME1*. Cells can grow on 5-flouroorotic acid if they no longer require a wild-type *NME1*. All plates were grown at 28 °C for 3–4 days. *A*, synthetic sick phenotype of *sic1*/*nme1* double mutants. *B*, synthetic sick phenotype of *nme1*, U2 components, and splicing proteins.

Ty1 levels are reduced over 5-fold in the RNase MRP mutant *nme1-Δ2* (Fig. 4*A*). This result is more consistent with RNase MRP playing a role in Ty1 maturation instead of stability. Improper assembly of a mature particle would be expected to produce lower levels of the Ty1 RNA.

DISCUSSION

Through the use of RIP-chip, we have identified several novel RNase MRP substrates. These additional substrates further implicate the critical role RNase MRP plays in cell cycle regulation. The identified substrates of RNase MRP share several common characteristics including roles in cell cycle progression, specific subcellular localization, and tight gene regulation. The identification of RNase MRP-associated TAM bodies and these newly identified substrates suggest that RNase MRP serves a specific role in the regulation of key transcripts, which may be asymmetrically distributed within the cell, to ensure proper cell division and continued cell viability (8).

These results place RNase MRP as a key player in the regulation of the spatiotemporal regulation of cell division by regulating key transcripts involved in the spatial positioning and resolution of cytokinesis. RNase MRP has been found in TAM bodies, cytoplasmic bodies that localize to the daughter cell prior to cytokinesis (8). It is in these TAM bodies that it is believed RNase MRP cleaves the *CLB2* transcript. Interestingly, the *CTS1* gene is also under cell cycle control and is asymmetrically expressed in daughter cells (31, 32). The synergistic effects of an RNase MRP/*xrn1* double mutant indicate that like the *CLB2* mRNA *CTS1* is processed in its 5′-UTR by RNase MRP to remove the cap and then rapidly degraded by the Xrn1 5′ to 3′ exonuclease (8). Sic1 is a cyclin/cyclin-dependent kinase inhibitor with high levels correlating with an exit from the cell cycle and low levels coinciding with cell cycle progression and an increased risk of cancer development in mammals (20). It is unclear why RNase MRP would process the *SIC1* mRNA if it is promoting cell cycle exit; however, degradation of this mRNA may help to fine-tune the next cell cycle in daughter cells along a temporal path different from that of the mother cell.

The finding that the U2 snRNA LSR1 is a substrate of RNase MRP is surprising and raises the possibility that RNase MRP might play a role in the biogenesis of ribonucleoproteins other than the ribosome. LSR1 may require a processing event by RNase MRP for full function and assembly. This is consistent with the synthetic sick phenotype seen between an RNase MRP RNA mutant and a deletion of either *LEA1* or *MSL1*. Both of these encode non-essential components of the U2 spliceosome. In addition, *PUS7* encodes a pseudouridine synthase that catalyzes the pseudouridylation of two positions in U2, and *DBR1* encodes the RNA lariat debranching enzyme important for intron turnover. Both the Dbr1 and Pus7 proteins have alternative functions (33), but the indication of U2 RNA as an RNase MRP substrate along with the *MSL1* and *LEA1* genetic interactions points to U2 as the root cause of the genetic interaction observed between these genes and the RNase MRP RNA *NME1*. We did not detect any accumulation of unspliced actin transcript in an RNase MRP mutant, but subtle transcript-specific splicing changes may still exist.

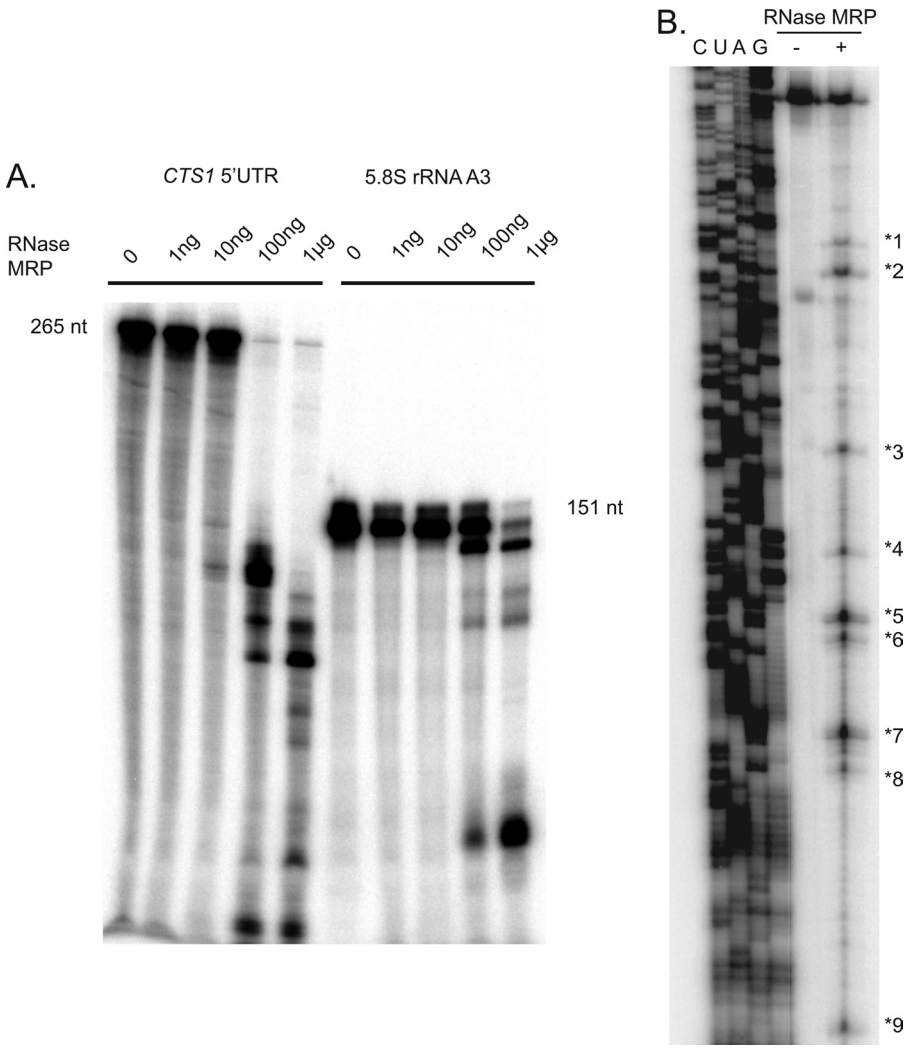

FIGURE 3. *A*, cleavage of *in vitro* transcribed *CTS1* 5′-UTR RNA and 5.8 S rRNA A3 by purified RNase MRP. 3′-End-labeled RNA of the 5.8 S rRNA A3 site was used as a positive control for RNase MRP cleavage activity. Similarly labeled *CTS1* 5′-UTR RNA was generated, and both were subjected to increasing amounts of RNase MRP enzyme for 30 min. *B*, determination of RNase MRP cleavage sites on the *CTS1* 5′-UTR. Cleavage products generated from *in vitro* transcribed *CTS1* 5′-UTR by purified RNase MRP were subjected to primer extension with CTS1-R3 primer and separated on a sequencing gel next to the *CTS1* 5′-UTR DNA sequence using the same primer. Positions of cleavage sites (**1–*9*) are indicated and are mapped in supplemental Fig. 1. *nt*, nucleotides.

Interestingly, the levels of *CTS1*, *SIC1*, and *LSR1* mRNAs were differentially affected in *nme1-Δ2 versus nme1-p6* mutants. This contrasts with the 5.8 S rRNA processing defects that are typically seen in both mutants, suggesting an allele-specific difference in substrate selection phenotypes. As the human homolog of *NME1*, *RMRP*, is mutated in cartilage-hair hypoplasia, these results may provide an understanding of the pleomorphic effects of RNase MRP mutants in humans (34). In addition, cartilage-hair hypoplasia patients have been found to exhibit an increased incidence of certain forms of cancer, which may be linked to cell cycle defects triggered by the failure of RNase MRP to process key cell cycle-regulated genes (35).

An unexpected result of this screen was the identification of a role for RNase MRP in Ty1 element transposition. This evidence is made even more interesting by the recent discovery that P-body elements are necessary for normal Ty1 transposition. P-bodies are cytoplasmic mRNA processing sites that like TAM bodies are sites of mRNA degradation. In addition, they share at least one common protein with TAM bodies (8, 36). Loss of P-body processing negatively effects Ty1 replication and thus transposition in yeast (37–39). Recently, RNase MRP has been found to play a role in viral RNA degradation of tomato bushy stunt virus when hosted in *S. cerevisiae* (40). Whether or not MRP is necessary for proper assembly of the Ty1 particle as may be the case with U2 or in degradation of the Ty1 RNA remains to be determined. The decrease in the levels of Ty1 RNA implies that RNase MRP is required in a processing event to stabilize and prevent degradation of the RNA by potentially promoting its assembly with particular proteins.

These results clearly implicate RNase MRP as a key enzyme not only in the maintenance of ribosomal RNA processing but also in the continued regulation of mitotic events. RNase MRP appears poised to degrade key transcripts in a specific subcellular space to help fine-tune the cell cycle. Moreover, RNase MRP appears to have been co-opted to help in the processing and maturation of other ribonucleoprotein particles in the cell (41). Additional research into this enzyme will undoubtedly reveal additional substrates and activities that will pro-

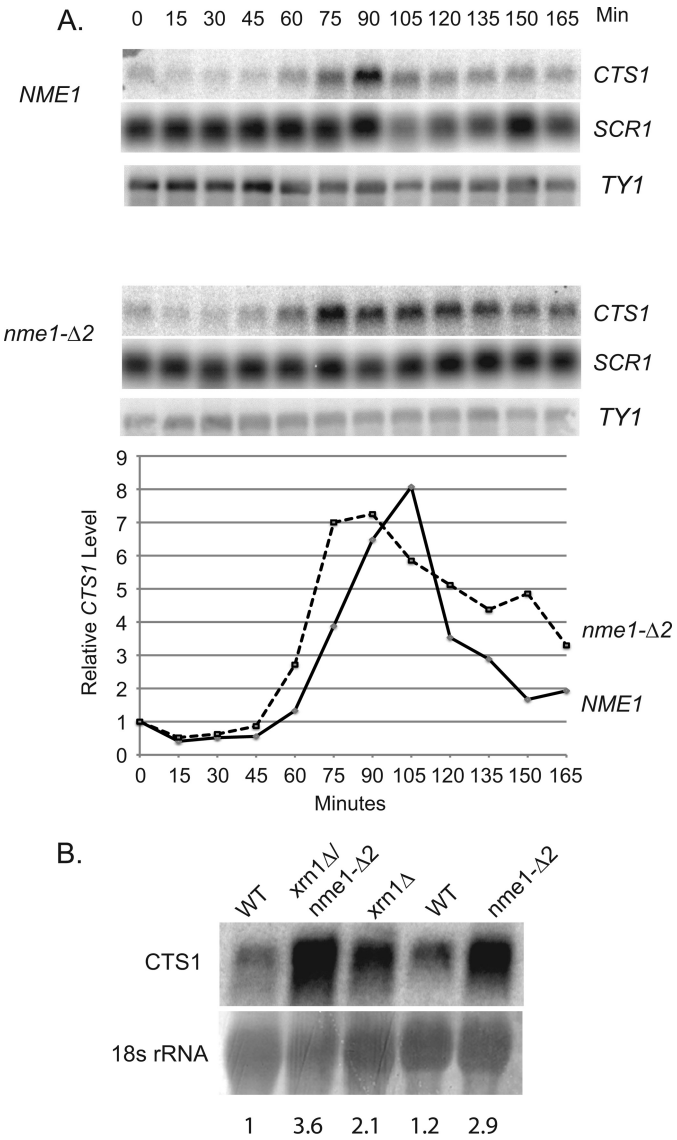

FIGURE 4. **Northern blot analysis of potential RNase MRP substrates.** *A*, Northern blot analysis of *CTS1* and Ty1 levels in synchronized *NME1* (wild-type) and *nme1-Δ2* strains. *NME1* and *nme1-Δ2* strains were synchronized by treatment with hydroxyurea, released, and then sampled every 15 min as indicated. *SCR1* levels were used as a loading control. Levels of CTS1 transcript were plotted and are relative to the *SCR1* and zero time points. *B*, Northern blot analysis of *CTS1* mRNA levels in wild type (*WT*), Δ*xrn1*, *nme1-Δ2*, and Δ*xrn1*/*nme1-Δ2* strains. Total RNA from wild type and the indicated mutants was separated on a formaldehyde-agarose denaturing gel, transferred, and probed for *CTS1*. Methylene blue staining of 18 S rRNA was used as a loading control. The -fold change in level from the control wild-type lane is indicated below the gel.

vide valuable insight into cell cycle regulation by RNase MRP and the development of the associated diseases in humans.

Acknowledgment—We are grateful to Qiaosheng Lu and M. D. Shafiuddin for careful reading of this manuscript.

REFERENCES

1. Salinas, K., Wierzbicki, S., Zhou, L., and Schmitt, M. E. (2005) Characterization and purification of *Saccharomyces cerevisiae* RNase MRP reveals a new unique protein component. *J. Biol. Chem.* **280,** 11352–11360
2. Houser-Scott, F., Xiao, S., Millikin, C. E., Zengel, J. M., Lindahl, L., and Engelke, D. R. (2002) Interactions among the protein and RNA subunits of *Saccharomyces cerevisiae* nuclear RNase P. *Proc. Natl. Acad. Sci. U.S.A.* **99,** 2684–2689
3. Schmitt, M. E., and Clayton, D. A. (1994) Yeast site-specific ribonucleoprotein endoribonuclease MRP contains an RNA component homologous to mammalian RNase MRP RNA and essential for cell viability. *Genes Dev.* **8,** 2617–2628
4. Forster, A. C., and Altman, S. (1990) Similar cage-shaped structures for the RNA components of all ribonuclease P and ribonuclease MRP enzymes. *Cell* **62,** 407–409
5. Schmitt, M. E., and Clayton, D. A. (1993) Nuclear RNase MRP is required for correct processing of pre-5.8S rRNA in *Saccharomyces cerevisiae*. *Mol. Cell. Biol.* **13,** 7935–7941
6. Lygerou, Z., Allmang, C., Tollervey, D., and Séraphin, B. (1996) The *POP1* gene encodes a protein component common to the RNase MRP and RNase P ribonucleoproteins. *Science* **272,** 268–270
7. Cai, T., Aulds, J., Gill, T., Cerio, M., and Schmitt, M. E. (2002) The *Saccharomyces cerevisiae* RNase mitochondrial RNA processing is critical for cell cycle progression at the end of mitosis. *Genetics* **161,** 1029–1042
8. Gill, T., Aulds, J., and Schmitt, M. (2006) A specialized processing body that is temporally and asymmetrically regulated during the cell cycle in *Saccharomyces cerevisiae*. *J. Cell Biol.* **173,** 35–45
9. Gill, T., Cai, T., Aulds, J., Wierzbicki, S., and Schmitt, M. E. (2004) RNase MRP cleaves the *CLB2* mRNA to promote cell cycle progression: novel method of mRNA degradation. *Mol. Cell. Biol.* **24,** 945–953
10. Chang, D. D., and Clayton, D. A. (1987) A novel endoribonuclease cleaves at a priming site of mouse mitochondrial DNA replication. *EMBO J.* **6,** 409–417
11. Li, K., Smagula, C. S., Parsons, W. J., Richardson, J. A., Gonzalez, M., Hagler, H. K., and Williams, R. S. (1994) Subcellular partitioning of MRP RNA assessed by ultrastructural and biochemical analysis. *J. Cell Biol.* **124,** 871–882
12. Thiel, C. T., Horn, D., Zabel, B., Ekici, A. B., Salinas, K., Gebhart, E., Rüschendorf, F., Sticht, H., Spranger, J., Müller, D., Zweier, C., Schmitt, M. E., Reis, A., and Rauch, A. (2005) Severely incapacitating mutations in patients with extreme short stature identify RNA-processing endoribonuclease RMRP as an essential cell growth regulator. *Am. J. Hum. Genet.* **77,** 795–806
13. Thiel, C. T., and Rauch, A. (2011) The molecular basis of the cartilage-hair hypoplasia-anauxetic dysplasia spectrum. *Best Pract. Res. Clin. Endocrinol. Metab.* **25,** 131–142
14. Jain, R., Devine, T., George, A. D., Chittur, S. V., Baroni, T. E., Penalva, L. O., and Tenenbaum, S. A. (2011) RIP chip analysis: RNA-binding protein immunoprecipitation-microarray (chip) profiling. *Methods Mol. Biol.* **703,** 247–263
15. Ule, J., Jensen, K., Mele, A., and Darnell, R. B. (2005) CLIP: a method for identifying protein-RNA interaction sites in living cells. *Methods* **37,** 376–386
16. Schmitt, M. E., Brown, T. A., and Trumpower, B. L. (1990) A rapid and simple method for preparation of RNA from *Saccharomyces cerevisiae*. *Nucleic Acids Res.* **18,** 3091–3092
17. Sambrook, J., MacCallum, P., and Russell, D. W. (2001) *Molecular Cloning: A Laboratory Manual*, 3rd Ed., Cold Spring Harbor Laboratory Press, Cold Spring Harbor, NY
18. Cai, T., Reilly, T. R., Cerio, M., and Schmitt, M. E. (1999) Mutagenesis of SNM1, which encodes a protein component of the yeast RNase MRP, reveals a role for this ribonucleoprotein endoribonuclease in plasmid segregation. *Mol. Cell. Biol.* **19,** 7857–7869
19. Shadel, G. S., Buckenmeyer, G. A., Clayton, D. A., and Schmitt, M. E. (2000) Mutational analysis of the RNA component of *Saccharomyces cerevisiae* RNase MRP reveals distinct nuclear phenotypes. *Gene* **245,** 175–184
20. Barberis, M., De Gioia, L., Ruzzene, M., Sarno, S., Coccetti, P., Fantucci, P., Vanoni, M., and Alberghina, L. (2005) The yeast cyclin-dependent kinase inhibitor Sic1 and mammalian p27Kip1 are functional homologues with a structurally conserved inhibitory domain. *Biochem. J.* **387,** 639–647
21. Stevens, S. W., Ryan, D. E., Ge, H. Y., Moore, R. E., Young, M. K., Lee, T. D., and Abelson, J. (2002) Composition and functional characterization of the yeast spliceosomal penta-snRNP. *Mol. Cell* **9,** 31–44

22. Chapman, K. B., and Boeke, J. D. (1991) Isolation and characterization of the gene encoding yeast debranching enzyme. *Cell* **65,** 483–492
23. Ma, X., Zhao, X., and Yu, Y. T. (2003) Pseudouridylation (ψ) of U2 snRNA in *S. cerevisiae* is catalyzed by an RNA-independent mechanism. *EMBO J.* **22,** 1889–1897
24. Nagalakshmi, U., Wang, Z., Waern, K., Shou, C., Raha, D., Gerstein, M., and Snyder, M. (2008) The transcriptional landscape of the yeast genome defined by RNA sequencing. *Science* **320,** 1344–1349
25. Yassour, M., Kaplan, T., Fraser, H. B., Levin, J. Z., Pfiffner, J., Adiconis, X., Schroth, G., Luo, S., Khrebtukova, I., Gnirke, A., Nusbaum, C., Thompson, D. A., Friedman, N., and Regev, A. (2009) *Ab initio* construction of a eukaryotic transcriptome by massively parallel mRNA sequencing. *Proc. Natl. Acad. Sci. U.S.A.* **106,** 3264–3269
26. Karwan, R., Bennett, J. L., and Clayton, D. A. (1991) Nuclear RNase MRP processes RNA at multiple discrete sites: interaction with an upstream G box is required for subsequent downstream cleavages. *Genes Dev.* **5,** 1264–1276
27. Lu, Q., Wierzbicki, S., Krasilnikov, A. S., and Schmitt, M. E. (2010) Comparison of mitochondrial and nucleolar RNase MRP reveals identical RNA components with distinct enzymatic activities and protein components. *RNA* **16,** 529–537
28. Esakova, O., Perederina, A., Quan, C., Berezin, I., and Krasilnikov, A. S. (2011) Substrate recognition by ribonucleoprotein ribonuclease MRP. *RNA* **17,** 356–364
29. O'Conallain, C., Doolin, M. T., Taggart, C., Thornton, F., and Butler, G. (1999) Regulated nuclear localisation of the yeast transcription factor Ace2p controls expression of chitinase (*CTS1*) in *Saccharomyces cerevisiae. Mol. Gen. Genet.* **262,** 275–282
30. Roth, J. F. (2000) The yeast Ty virus-like particles. *Yeast* **16,** 785–795
31. Doolin, M. T., Johnson, A. L., Johnston, L. H., and Butler, G. (2001) Overlapping and distinct roles of the duplicated yeast transcription factors Ace2p and Swi5p. *Mol. Microbiol.* **40,** 422–432
32. Ufano, S., Pablo, M. E., Calzada, A., del Rey, F., and Vazquez de Aldana, C. R. (2004) Swm1p subunit of the APC/cyclosome is required for activation of the daughter-specific gene expression program mediated by Ace2p during growth at high temperature in *Saccharomyces cerevisiae. J. Cell Sci.* **117,** 545–557
33. Behm-Ansmant, I., Urban, A., Ma, X., Yu, Y. T., Motorin, Y., and Branlant, C. (2003) The *Saccharomyces cerevisiae* U2 snRNA:pseudouridine-synthase Pus7p is a novel multisite-multisubstrate RNA:ψ-synthase also acting on tRNAs. *RNA* **9,** 1371–1382
34. Ridanpää, M., van Eenennaam, H., Pelin, K., Chadwick, R., Johnson, C., Yuan, B., vanVenrooij, W., Pruijn, G., Salmela, R., Rockas, S., Mäkitie, O., Kaitila, I., and de la Chapelle, A. (2001) Mutations in the RNA component of RNase MRP cause a pleiotropic human disease, cartilage-hair hypoplasia. *Cell* **104,** 195–203
35. Taskinen, M., Ranki, A., Pukkala, E., Jeskanen, L., Kaitila, I., and Mäkitie, O. (2008) Extended follow-up of the Finnish cartilage-hair hypoplasia cohort confirms high incidence of non-Hodgkin lymphoma and basal cell carcinoma. *Am. J. Med. Genet. A* **146A,** 2370–2375
36. Sheth, U., and Parker, R. (2006) Targeting of aberrant mRNAs to cytoplasmic processing bodies. *Cell* **125,** 1095–1109
37. Aye, M., Irwin, B., Beliakova-Bethell, N., Chen, E., Garrus, J., and Sandmeyer, S. (2004) Host factors that affect Ty3 retrotransposition in *Saccharomyces cerevisiae*. *Genetics* **168,** 1159–1176
38. Larsen, L. S., Beliakova-Bethell, N., Bilanchone, V., Zhang, M., Lamsa, A., Dasilva, R., Hatfield, G. W., Nagashima, K., and Sandmeyer, S. (2008) Ty3 nucleocapsid controls localization of particle assembly. *J. Virol.* **82,** 2501–2514
39. Larsen, L. S., Zhang, M., Beliakova-Bethell, N., Bilanchone, V., Lamsa, A., Nagashima, K., Najdi, R., Kosaka, K., Kovacevic, V., Cheng, J., Baldi, P., Hatfield, G. W., and Sandmeyer, S. (2007) Ty3 capsid mutations reveal early and late functions of the amino-terminal domain. *J. Virol.* **81,** 6957–6972
40. Jaag, H. M., Lu, Q., Schmitt, M. E., and Nagy, P. D. (2011) Role of RNase MRP in viral RNA degradation and RNA recombination. *J. Virol.* **85,** 243–253
41. Maida, Y., Yasukawa, M., Furuuchi, M., Lassmann, T., Possemato, R., Okamoto, N., Kasim, V., Hayashizaki, Y., Hahn, W. C., and Masutomi, K. (2009) An RNA-dependent RNA polymerase formed by TERT and the RMRP RNA. *Nature* **461,** 230–235